peak current density of 8.9 kA/cm^2 was obtained for an unstrained AlInAsSb/InGaAs double-barrier resonant tunneling diode.

REFERENCES

[1] L. L. Chang, L. Esaki, and R. Tsu, "Resonant tunneling in semiconductor double barriers," *Appl. Phys. Lett.*, vol. 24, pp. 593–595, 1974.

[2] T. J. Shewchuk *et al.*, "Resonant tunneling oscillations in GaAs-$Al_xGa_{1-x}As$ heterostructure at room temperature," *Appl. Phys. Lett.*, vol. 46, pp. 508–510, 1985.

[3] C. I. Huang *et al.*, "AlGaAs/GaAs double barrier diodes with high peak-to-valley current ratio," *Appl. Phys. Lett.*, vol. 51, pp. 121–123, 1987.

[4] M. Tsuchiya, H. Sakaki, and J. Yoshino, "Room temperature observation of differential negative resistance in an AlAs/GaAs/AlAs resonant tunneling diode," *Jpn J. Appl. Phys.*, vol. 24, pp. L446–L468, 1985.

[5] M. Tsuchiya and H. Sakaki, "Dependence of resonant tunneling current on well widths in AlAs/GaAs/AlAs double barrier diode structures," *Appl. Phys. Lett.*, vol. 49, pp. 88–90, 1986.

[6] T. Inata *et al.*, "Excellent negative differential resistance of InAlAs/InGaAs resonant tunneling barrier structures grown by MBE," *Jpn. J. Appl. Phys.*, vol. 25, pp. L983–L985, 1986.

[7] Y. Sugiyama *et al.*, "Current-voltage characteristics of $In_{0.53}Ga_{0.47}As/In_{0.52}Al_{0.48}As$ resonant tunneling barrier structures grown by molecular beam epitaxy," *Appl. Phys. Lett.*, vol. 52, pp. 314–316, 1988.

[8] J. H. Smet, T. P. E. Broekaert, and C. G. Fonstad, "Peak-to-valley current ratios as high as 50:1 at room temperature in pseudomorphic $In_{0.53}Ga_{0.47}As$/AlAs/InAs resonant tunneling diodes," *J. Appl. Phys.*, vol. 71, pp. 2475–2477, 1992.

[9] J. S. Su, W. C. Hsu, W. Lin, and S. Y. Jain, "High-breakdown characteristics of the InP-based heterostructure field-effect transistor with $Al_{0.66}In_{0.34}As_{0.85}Sb_{0.15}$ Schottky layer," *IEEE Electron Device Lett.*, vol. 19, pp. 195–197, 1998.

[10] G. Bastard, "Theoretical investigations of superlattice band structure in the envelope function approximation," *Phys. Rev. B*, vol. 25, pp. 7584–7597, 1982.

[11] L. Hrivnák, "Exciton binding energy as a function of the well width," *J. Appl. Phys.*, vol. 72, pp. 3218–3219, 1992.

[12] R. People, K. W. Wecht, K. Alavi, and A. Y. Cho, "Measurement of the conduction-band discontinuity of molecular beam epitaxial grown $In_{0.52}Al_{0.48}As/In_{0.53}Ga_{0.47}As$ N-n heterojunction by C/V profiling," *Appl. Phys. Lett.*, vol. 43, pp. 118–120, 1983.

[13] Y. Sugiyama *et al.*, "Conduction band edge discontinuity of $In_{0.52}Ga_{0.48}As/In_{0.52}(Ga_{1-x}Al_x)_{0.48}As$ $(0 \leqq cx \leqq 1)$ heterostructures," *Jpn. J. Appl. Phys.*, vol. 25, pp. L648–L650, 1986.

[14] L. Bornstein, *Numerical Data and Functional Relationships in Science and Technology*, O. Madelung, M. Schulz, and H. Weiss, Eds. Berlin, Germany: Springer-Verlag, 1982, vol. 17a and 17b.

[15] S. Adachi, "Band gaps and refractive indices of AlGaAsSb, GaInAsSb, and InPAsSb: Key properties for a variety of the 2–4-μm optoelectronic device applications," *J. Appl. Phys.*, vol. 61, pp. 4869–4876, 1987.

[16] R. People and S. A. Jackson, *Semiconductors and Semimetals*, T. P. Pearsall, Ed. New York: Academic, 1990, vol. 32, p. 154.

[17] J. I. Pankove, *Optical Process in Semiconductors*. Englewood Cliffs, NJ: Prentice-Hall, 1971, p. 412.

[18] A. D. Andreev and G. G. Zegrya, "Theoretical study of thresholdless Auger recombination in compressively strained InAlAsSb/GaSb quantum wells," *Appl. Phys. Lett.*, vol. 70, pp. 601–603, 1997.

[19] P. W. Yu *et al.*, "High valence-band offset of GaSbAs-InAlAs quantum wells grown by molecular beam epitaxy," *Appl. Phys. Lett.*, vol. 61, pp. 2317–2319, 1992.

Theory of the Single Contact Electron Beam Induced Current Effect

V. K. S. Ong, K. T. Lau, and J. G. Ma

***Abstract*—All publications on the single contact electron beam induced current (SC-EBIC) technique so far have been concerned with the application of the technique. This paper seeks to examine the theory behind the technique and supports it with experimental observation. It will be shown that the technique can be used, not only on electron and ion beam machines, but also on any scanning equipment that is capable of generating electron-hole pairs within a semiconductor device, e.g., with the use of a fine laser beam.**

***Index Terms*—Displacement current, EBIC, electric displacement , electromagnetics, SC-EBIC, SEM.**

I. INTRODUCTION

It has been shown recently that it is possible to capture electron beam induced current (EBIC) images of integrated circuit (IC's) using only a single contact, as opposed to the multiple contacts required by the traditional EBIC technique [1], [2]. This new technique is called the *single contact electron beam induced current technique* or SC-EBIC. An example of a micrograph captured by this technique is shown in Fig. 1. It was also shown in [1] and [2] that EBIC images of entire IC's can be captured using this method and that it was possible to use it to detect device failures. This same technique was also used successfully on ion beam machines [3], [4].

Traditional EBIC requires that a complete electrical circuit be formed across a junction that is to be imaged. For every extra junction that needs to be imaged, an additional connection needs to be made on the semiconductor. For a magnified image of a small area of an IC, which may have hundreds of junctions, more than that number of connections need to be made on the IC. This is not only unfeasible in practice, but the connections, which is normally made with probe pins [5]–[7], will block the electron beam and prevent it from reaching the IC, causing massive shadowing.

The idea behind the technique described in [1]–[4] is to completely remove all but one of the probes. This is possible in the transient mode since the circuit, which is traditionally completed by the second probe, is now replaced by the displacement current created by the transient.

II. SC-EBIC EXPERIMENT FOR A SINGLE JUNCTION

A simple SC-EBIC experiment is set up by wiring up a piece of semiconductor sample with a single metallurgical junction fabricated on it as shown in Fig. 2. At time $t_{\rm on}$, say, an electron beam is turned on to impinge directly upon the junction. A few tens of milliseconds later, the beam is turned off. The current measured by the current meter is then plotted against time. The result is shown in Fig. 3.

III. SC-EBIC THEORY FOR A SINGLE JUNCTION

Consider a single semiconductor junction connected as shown in Fig. 2. The device is initially in thermal equilibrium. Under this condition the current meter registers a zero current. At time $t_{\rm on}$, a beam

Manuscript received October 6, 1998; revised February 12, 1999. The review of this paper was arranged by Editor J. N. Hollenhorst.

The authors are with the School of Electrical and Electronic Engineering, Nanyang Technological University, Nanyang Avenue, Singapore 639798, Republic of Singapore (e-mail: eongks@ntu.edu.sg).

Publisher Item Identifier S 0018-9383(00)00172-6.

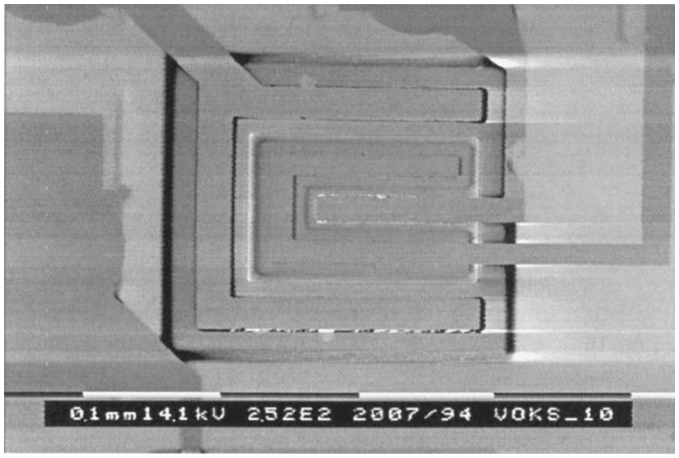

Fig. 1. Example of an SC-EBIC image.

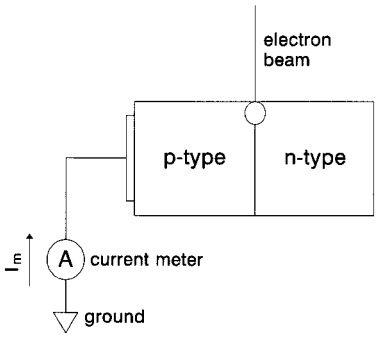

Fig. 2. Single function SC-EBIC configuration.

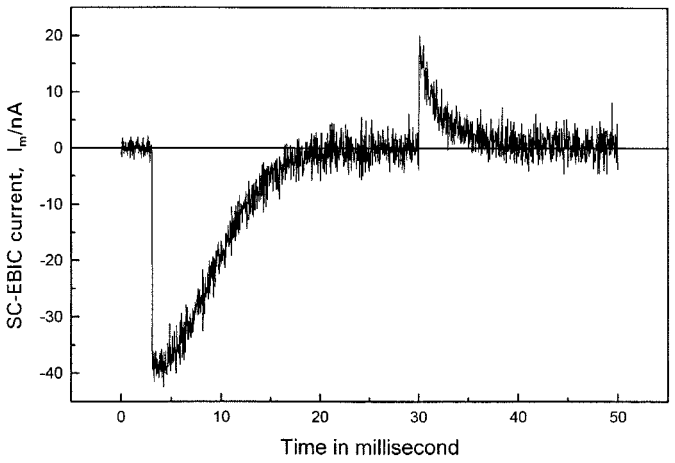

Fig. 3. Graph of a single junction SC-EBIC experiment.

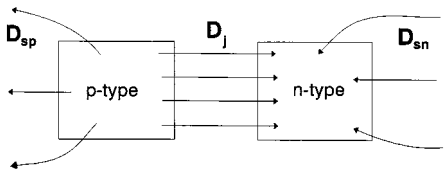

Fig. 4. Displacement vectors.

of electrons begins to impinge upon the semiconductor junction. Electrons entering into the semiconductor will ionize the material and generate electron-hole pairs (EHP's). The electric field at the junction is such that the holes and electrons drift towards the p- and n-type regions, respectively.

The p-type region has a short-circuit to ground through the current meter, and is therefore always at ground potential. The n-type region, however, is floating. The beam generated electrons that are swept by the electric field into the n-type region will therefore be trapped and accumulates in the n-type region. These negatively charged electrons accumulating in the n-type region will cause two groups of electric displacements to terminate into it. This is illustrated in Fig. 4, where the space charge region (SCR) is removed. The first group of electric displacements, denoted as $\boldsymbol{D}_j$ in Fig. 4, are those which originate from the accumulation of positively charged holes in the p-type region. The second group, denoted as $\boldsymbol{D}_{sn}$ in Fig. 4, are the electric displacements which originate from nearby ground planes, e.g., the objective lens pole piece and housing of the SEM, and the grounded specimen holder.

The rate of change of this second group of electric displacements give rise to displacement currents flowing from the nearby ground planes into the n-type region [8]. This displacement current is balanced by an equal amount of electric current flowing from the p-type region to ground through the current meter. This explains the initial flow of current at $t_{\rm on} = 3$ ms in Fig. 3.

As the electrons accumulate in the n-type region, the strength of the electric displacements also increases. This increase in electric displacement will cause the potential of the n-type region to fall. This in turn causes the junction electric field to weaken, and the junction will begin to conduct in the forward direction.

As the junction forward biases, electrons get injected from the n-type region into the p-type region, hence the rate of electrons accumulating in the n-type region decreases. This reduces the rate of change of the second group of electric displacements, $\boldsymbol{D}_{sn}$ in Fig. 4, which directly decreases the displacement currents flowing into the n-type region from the nearby ground planes. Consequently, this reduction in the displacement current is balanced by a reduced flow of electric current out of the p-type region to ground through the current meter. This explains the reduced flow of SC-EBIC current in Fig. 3 between $t_{\rm on}$ and $t = 20$ ms.

An equilibrium takes place between 20–30 ms in the graph of Fig. 3. This is when the generation current due to EHP creation by the electron beam and separation by the junction electric field balances the forward bias current in the junction. As a result of this balance, the accumulated electrons in the n-type region neither increase nor decrease. The electric displacements from nearby ground planes terminating in the n-type region, $\boldsymbol{D}_{sn}$, therefore become constant, and the displacement current, which is the partial time derivative of this electric displacement, vanishes. The zero displacement current is consequently balanced by zero SC-EBIC current flowing through the current meter. However, the constant electron beam current itself continues to flow through the current meter. This current is about 0.1 nA, and therefore cannot be readily seen in Fig. 3.

When the electron beam is removed from the junction at time $t_{\rm off}$, the generation current suddenly disappears. This causes a sudden change from an equilibrium state where the accumulated electrons in the n-type region neither increase nor decrease, to a state in which the depletion rate of the accumulated electrons in the n-type region equals the junction forward bias current. This change consequently gives rise to displacement currents flowing from the n-type region to the nearby ground planes (opposite in direction to $\boldsymbol{D}_{sn}$), which is again balanced by the SC-EBIC current flowing from the ground to the p-type region through the current meter. This can be seen in Fig. 3 where $t_{\rm off} = 30$ ms.

As electrons from the n-type region continues to inject into the p-type region, the amount of accumulated electrons in the n-type region decreases. This causes the electric displacements to also decrease, resulting in a rise in the potential of the n-type region. This in turn causes the junction to be less and less strongly forward biased. The rate of de-

crease of the accumulated electrons decreases, resulting in a decrease in the displacement current flowing from the n-type region to ground. The SC-EBIC current which balances the displacement current also decreases, as can be seen in Fig. 3 from $t_{\rm off} = 30$ ms onwards.

It is to be noted that since the junction becomes less and less strongly forward biased as electrons flow out of the n-type region, the rate of the flow of electrons also decreases in a very gradual manner. Although it is not obvious in Fig. 3, the SC-EBIC current in this figure does not actually become zero at the 40 ns mark. It continues on asymptotically.

If one were to look closely at Fig. 3, it can be seen that the wiggly line lies mainly above the zero current line. This effect can also be seen in Fig. 1, where the white streaks continue on strongly right through the right hand edge of the micrograph. It is important to note here that the areas under the curve of Fig. 3 before and after $t_{\rm off}$ must be equal if one were to plot it for a few hundred ms, since each of these areas represent the total amount of excess charge stored in the n-type region.

It is also to be noted that the entire process described above sits on top of the generation and recombination processes that are going on in the semiconductor. The process described above is mainly electromagnetic in nature, and is therefore a function of the excess charges which accumulate in the n-type region. These excess charges are not affected by the generation and recombination processes since the n-type region is floating in the electrical sense.

The time constant of the entire measurement circuit has been measured to be of the order of about half a microsecond. This is about four orders of magnitude better than the time constants in the graph of Fig. 3. In fact the superior time constant of the measurement circuit is self evident from the fact that the electrical noise is reproduced quite faithfully by the measurement circuit in Fig. 3. If the time constant of the measurement circuit had been significantly poorer, then the electrical noise would have been smoothed out.

The explanation for the SC-EBIC phenomenon given above assumes the use of energetic electrons to generate the EHP's. It can be seen that the explanation given above is similarly valid, regardless of the means of generating the EHP's. So far, the technique has be used successfully with electron and ion beams. Successful preliminary experiments have been conducted with the use of laser beam.

IV. Conclusion

The explanation behind the SC-EBIC effect was described in this article using well known electromagnetics theory. It was shown that the explanation agrees qualitatively with experiment. It is hoped that this will fill up the void in the literature on the SC-EBIC effect.

Acknowledgment

A part of this work was done at the National University of Singapore. V. K. S. Ong would like to acknowledge interesting discussions with D. S. H. Chan and J. C. H. Phang on this work.

References

[1] V. K. S. Ong, J. C. H. Phang, and D. S. H. Chan, "Novel EBIC observation of unconnected junctions of large area VLSI circuits," in *Proc. 20th Int. Symp. Testing and Failure Analysis*, Los Angeles, CA, Nov. 1994, pp. 49–56.

[2] V. K. S. Ong, P. C. Liu, and K. T. Lau, "Large area electron beam induced current imaging with a single contact," *Solid-State Electron.*, vol. 43, pp. 17–25, Jan. 1999.

[3] S. Kolachina *et al.*, "Ion beam induced charge (IBIC) imaging for the failure analysis of multi-level metal VLSI circuits," in *Proc. 21st Int. Symp. Testing and Failure Analysis*, Santa Clara, CA, Nov. 1995, pp. 19–24.

[4] S. Kolachina *et al.*, "Unconnected junction contrast in ion beam induced charge microscopy," *Appl. Phys. Lett.*, vol. 68, pp. 532–534, 1996.

[5] C. Coakley and A. Marquez, "Microprobing and EBIC for VLSI technology," in *Proc. 18th Int. Symp. Testing and Failure Analysis*, Los Angeles, CA, 1992, pp. 43–48.

[6] E. Hutchinson, "CMOS characterization using EBIC: Applications and performance," in *Proc. 17th Int. Symp. Testing and Failure Analysis*, Santa Clara, CA, 1991, pp. 199–204.

[7] G. V. Lukianoff, "Beam-induced current testing in the line support environment," in *Electron Beam Testing Technology*, J. T. L. Thong, Ed. New York: Plenum, 1993, pp. 433–444.

[8] D. K. Cheng, *Field and Wave Electromagnetics*. Boston, MA: Addison-Wesley, 1989.